

Estimation of viscosity of natural salts of the Hormuz- and the Namakdan salt diapirs in the Persian Gulf

Soumyajit Mukherjee¹, Christopher Talbot², and Hemin A Koyi²

¹ Indian Institute of Technology Roorkee, Rooree-247667, Uttarakhand, INDIA.
² Hans Ramberg Tectonic Laboratory, Uppsala University, Uppsala 752 36, SWEDEN

ABSTRACT

The Hormuz- and the Namakdan salt diapirs extrude as parabolic profiles in the last 10^4 years. Velocity profiles of salts extruding through these diapirs are derived assuming Newtonian viscous flow of salts. Viscosity of salt in these diapirs are calculated to be 10^{18} - 10^{21} Pa s and 10^{17} - 10^{21} Pa s, respectively.

INTRODUCTION

Rocks under high stress over a short time span, at shallow crustal depth, may undergo brittle deformation. If the stress persists for a longer time span of geological significance, such as thousands of years due to tectonic reasons, rocks undergo ductile deformation. Estimation of the rheological parameters of the rocks is of fundamental importance in material science and in civil engineering. Most of the studies in rock rheology are confined to the brittle regime since brittle deformation of rocks is easy to perform over short time-span, and is also suitable in laboratories. On the other hand, parameters of ductility of rocks, most significantly the viscosity, are not possible to measure in the laboratory. Geoscientists have occasionally estimated viscosity of rocks by comparing the model deformation pattern with that in the real rocks. The viscosity data so obtained are useful in further tectonic modelling at different scales.

Most of the 200 or so diapirs of Hormuz salt in the Zagros mountains of Iran extrude mountains of salt that rise 400 m above their vents in strong limestones before they gravity spread as viscous fountains. Bruthans et al.¹ demonstrated that seven of the eight local rise rates constrained for the Hormuz Island, and all the local rates on the Namakdan, fit well with the parabolic curves expected for the extrusion of a Newtonian viscous fluid from a cylindrical channel.

Based on the data of uplift rate of Bruthans et al.¹ and the velocity profiles we deduce in this work, we estimate of the dynamic viscosities of the salts of the Hormuz- and Namakdan salt diapirs from the Persian Gulf.

METHODOLOGIES

The pressure exerted on the Hormuz salt by the surrounding country rock (mainly limestones) is taken as the mechanism of extrusion of the Hormuz- and the Namakdan diapirs. The pressure exerted downwards by the extruded salt modifies the pressure gradient driving the extrusion, and is used to deduce the velocity profiles of the extrusive salt through elliptical- (Eqs 20 & -22) and circular (Eqs 23 & -24) planforms of the diapirs. These derivations assume that the extruded salt does not undergo gravitational spreading. We use the first set of equations to estimate the dynamic viscosity (μ) of the

salt of the Hormuz diapir (Table 1), and the second set to deduce that for the Namakdan diapir (Table-2).

In these calculations, the coordinates of the locations of known uplift rates (the (x,y) ordinates in Table 1) were calculated and used after taking the center of the Hormuz diapir (Fig. 2 of Bruthans et al.¹), as the origin of the coordinate axes (and also the origin of the major- and the minor axes of the elliptical outcrop). The extrusion rates [$U_z(y,z,t)$, $U_z(y_1,t)$,] used in the calculations are obtained from 7 data points for the Hormuz- and 6 data points for the Namakdan diapir (from Fig. 9a and -b of Bruthans et al.¹).

RESULTS

The dynamic viscosity of the salt in the Hormuz diapir lies in the range of 10^{18} - 10^{21} Pa s considering its extrusion through elliptical planform. The viscosity of the salt in the Namakdan diapir has been estimated by approximating its sub-circular planform as circular. The calculated range, 10^{17} - 10^{21} Pa s, of its extruded salt is expected to represent approximately that extruded from the elliptical planform. This is because of the fact that the planform of the Namakdan diapir has very low ellipticity and very high sphericity (ellipticity: $e=m.n^{-1}=1.03$; sphericity: $S_p=2.(mn^2)^{1/3} \cdot \{m+9.(m^2-n^2)^{1/2} \cdot \ln((m+(m^2-n^2)^{1/2})/3)\}^{-1} \sim 1.0$; calculated from m (major axis) =7km and n (minor axis) =6.8km as given in Bruthans et al.¹).

APPENDIX

The 'Poisson equation' of rectilinear flow of a Newtonian viscous fluid in the z-direction in an infinitely long parallel-wall inclined channel is given by:

$$(\partial^2 U_z / \partial x^2) + (\partial^2 U_z / \partial y^2) = \mu^{-1} [(\partial P / \partial x) - d_1 \cdot g \cdot \sin \theta] \quad (1)$$

(Same as Eq 6.190 of Papanastasiou et al.², but with symbols as per our choice)

Here the x- and the y-directions are mutually perpendicular, both perpendicular to the z-axis, and lie on the planform of the channel; ' μ ' is the dynamic viscosity of the fluid; $(\partial P / \partial x)$ is the pressure gradient acting on the fluid along the x-direction; ' d_1 ' is the density of the fluid, ' g ' is the acceleration due to gravity, and ' θ ' is the inclination of the channel.

We now consider (i) the channel to be very long but of finite length; (ii) the channel to be vertical; (iii) the fluid rise within the channel due to pressure exerted by the surrounding overburden of higher density d_2 ($d_2 > d_1$) on the horizontal source layer; and (iv) the planform of the channel to be elliptical with 'x' and 'y' as the major- and the minor axes, and of lengths '2a' and '2b', respectively (Fig. 2). Because of constraint (i),

$$d_1 \cdot g \cdot \sin \theta = d_1 \cdot g.$$

Applying this and the constraint (ii),

$$(\partial P / \partial x) = [d_2 \cdot g - P_{out}(t) \cdot H^{-1}]$$

where $P_{out}(t)$ stands for the pressure exerted by the extruded fluid on the surface over which it has extruded. Therefore, the resultant pressure gradient acting vertically upwards on the fluid column 'A', at depth H is,

$$[(\partial P / \partial x) - d \cdot g \cdot \sin \theta] = [g \cdot (d_2 - d_1) - P_{out}(t) \cdot H^{-1}].$$

Thus, Eq (1) becomes

$$(\partial^2 U_z / \partial x^2) + (\partial^2 U_z / \partial y^2) = \mu^{-1} \cdot \{g \cdot (d_2 - d_1) - P_{out}(t) \cdot H^{-1}\} \quad (2)$$

Let $U_z(x,y,t)$ be the velocity of the extruding fluid at coordinate (x,y) at instant $t=t$. Considering the channel walls to be static during fluid flow, the boundary condition is

$$U_z(x,y,t)=0, \quad \text{at } (x^2 \cdot a^{-2} + y^2 \cdot b^{-2})=1 \quad (3)$$

A dependent variable U_z' is now introduced such that

$$U_z(x,y,t)=U_z'(x,y,t)+c_1x^2+c_2y^2 \quad (4)$$

c_1, c_2 are constants, $\neq 0$, and are to be solved so that the following conditions are satisfied: (i) $U_z'(x,y,t)$ satisfies the Laplace equation, and (ii) $U_z'(x,y,t)$ is constant on the wall at a particular instant 't'. Substituting Eq (4) into Eq (2):

$$(\partial^2 U_z'/\partial x^2) + (\partial^2 U_z'/\partial y^2) + 2(c_1 + c_2) = \mu^{-1} \cdot \{(d_2 - d_1) \cdot g - P_{out}(t) \cdot H^{-1}\} \quad (5)$$

$U_z'(x)$ will satisfy the Laplace Equation:

$$(\partial^2 U_z'/\partial x^2) + (\partial^2 U_z'/\partial y^2) = 0 \quad (6)$$

if

$$2(c_1 + c_2) = \mu^{-1} \cdot \{(d_2 - d_1) \cdot g - P_{out}(t) \cdot H^{-1}\} \quad (7)$$

From the boundary condition (Eq 3):

$$U_z'(x,y,t) = -(c_1x^2 + c_2y^2) = -c_1(x^2 + c_2 \cdot c_1^{-1} \cdot y^2) \quad (8)$$

$$\text{at } (x^2 \cdot a^{-2} + y^2 \cdot b^{-2})=1$$

Fixing

$$(c_2 \cdot c_1^{-1}) = (a^2 \cdot b^{-2}) \quad (9)$$

$U_z'(x,y,t)$ is constant at the channel boundary at a particular instant 't':

$$U_z'(x,y,t) = -c_1a^2 \text{ on } (x^2 \cdot a^{-2} + y^2 \cdot b^{-2})=1 \quad (10)$$

According to the maximum principle for the Laplace equation, $U_z'(x,y,t)$ has both its minimum and maximum values on the boundary of the domain. This means that $U_z'(x,y,t)$ is constant over the whole domain at a particular time:

$$U_z'(x,y,t) = -c_1a^2 \quad (11)$$

Putting Eq (11) in eq (4), and using eq (9)

$$U_z(x,y,t) = (-c_1a^2 + c_1x^2 + c_2y^2) = -c_1a^2(1 - x^2a^{-2} - c_2c_1^{-1}y^2a^{-2}) \quad (12)$$

or,

$$U_z(x,y,t) = -c_1a^2(1 - x^2a^{-2} - y^2b^{-2}) \quad (13)$$

The constant c_1 is obtained from Eq (7) and Eq (9)

$$c_1 = 0.5 \cdot b^2 \cdot \mu^{-1} \cdot \{(d_2 - d_1) \cdot g - P_{out}(t) \cdot H^{-1}\} \cdot (a^2 + b^2)^{-1} \quad (14)$$

Putting the c_1 value of Eq (14) into Eq (13):

$$U_z(x,y,t) = -0.5 \cdot \mu^{-1} \cdot \{(d_2 - d_1) \cdot g - P_{out}(t) \cdot H^{-1}\} \cdot (a^2b^2) \cdot (a^2 + b^2)^{-1} \cdot (1 - x^2 \cdot a^{-2} - y^2 \cdot b^{-2}) \quad (15)$$

Now, integration of the velocity profile given by Eq (15) over the elliptical planform gives the volumetric flow rate

$$Q(t) = -0.25 \cdot \pi \cdot a^3b^3 \cdot \mu^{-1} \cdot \{(d_2 - d_1) \cdot g - P_{out}(t) \cdot H^{-1}\} \cdot (a^2 + b^2)^{-1} \quad (16)$$

In Eq (16) and onwards, we assume that no gravitational spreading of the extruded salt takes place. In other words, no part of the extruded salt is considered to go outside the planform. Now, dividing $Q(t)$ by the area of the elliptical cross-section ($A = \pi \cdot ab$) gives the volumetric flow rate per unit area as

$$Q'(t) = Q(t) \cdot A^{-1} = -0.25 \cdot a^2b^2 \cdot \mu^{-1} \cdot \{(d_2 - d_1) \cdot g - P_{out}(t) \cdot H^{-1}\} \cdot (a^2 + b^2)^{-1} \quad (17)$$

Equating $Q'(t)$ with the pressure buildup in extrusion gives

$$dP_{out}(t)/dt = Q'(t) \cdot d_1 \cdot g = -0.25 \cdot a^2b^2 \cdot d_1 \cdot g \cdot \mu^{-1} \cdot \{(d_2 - d_1) \cdot g - P_{out}(t) \cdot H^{-1}\} \cdot (a^2 + b^2)^{-1} \quad (18)$$

The solution of Eq (18) with the boundary condition $P(0)=0$ is

$$P_{out}(t)=g.(d_2-d_1).[1-\exp(-t.\tau^{-1})] \quad (19)$$

Where the ‘characteristic time’ (τ) has the following form

$$\tau=[4.\mu.H.a^{-2}b^{-2}.d_1^{-1}.g^{-1}.(a^2+b^2)] \quad (20)$$

Expanding the exponential series, neglecting terms higher than the second order, Eq (19) becomes

$$P_{out}(t)=g.(d_2-d_1).[1-t.\tau^{-1}] \quad (21)$$

Substituting this value of $P_{out}(t)$ of Eq (21) into Eq (15), and neglecting the negative sign at the right hand side

$$U_z(x,y,t)=0.5.g.\mu^{-1}.(d_2-d_1).(a^2b^2).(a^2+b^2)^{-1}.(1-x^2.a^{-2}-y^2.b^{-2}).(1-t.\tau^{-1}) \quad (22)$$

the absolute value of velocity, $U_z(x,y,t)$, is obtained. For circular planforms, putting $a=b=y_0$, the radius of the circle; and

$$y_1=(x^2+y^2)^{0.5},$$

the distance from the center; the velocity profile, given by Eq (22), simplifies to

$$U_z(y_1,t)=0.25.g.\mu^{-1}.(d_2-d_1).(y_0^2-y_1^2).(1-t.\tau^{-1})$$

The ‘characteristic time’, in this case, simplifies to

$$\tau=[8.\mu.H.y_0^{-2}.d_1^{-1}.g^{-1}] \quad (24)$$

Note that, until Eq (15), our derivation follows steps similar to Papanastasiou et al.², and our derivation from Eq (16) till Eq (22) follows Weinberger et al.³ while maintaining the physical boundary conditions appropriate for our problem.

The extrusion parameters and the channel geometry of the diapiric salt are

equated with those of the fluid in channel ‘A’ as follows.

- $U_z(x,y,t)$: velocity of the extruded salt at the coordinate (x,y) at instant ‘t’; for extrusion through an elliptical planform; symbol used in Eq (23) and in Table-1.
- τ : the ‘characteristic time’ of salt extrusion (cf. Weinberger et al.³), for both the elliptical and circular cross-sections of the diapir as used in Eqs (20) and (24), respectively.
- $U_z(y_1,t)$: velocity of the extruded salt at distance y_1 from the diapir center and at instant ‘t’, for extrusion through circular section; symbol used in Eq (23) and in Table 2.
- 2a, 2b: length of the major- and the minor axes of the elliptical outcrop of the diapir; 8.5km and 6.8km respectively for the Hormuz salt diapir (Bruthans et al.¹).
- $2y_0$: channel diameter, considering the circular cross-section; symbol used in Eq (23). In different considerations, the diameters are considered as the major- and minor axes of the elliptical outcrops of the diapirs (for the Hormuz diapir: $2y_0=8.5\text{km}$, 6.8km ; and for the Namakdan diapir: $2y_0=7\text{km}$, 6.8km , from Bruthans et al.¹).
- μ : dynamic viscosity of the diapiric salts; symbol used in Eqs (20) to (24).
- d_1, d_2 : density of salt and that of the limestone, whose natural ranges are between 2.0-2.2 c.c. and 2.37-2.8 c.c., respectively⁴. This gives $d_{\max \text{ diff}} = (d_2-d_1)_{\max} = 0.8 \text{ c.c.}$ (for $d_1=2 \text{ c.c.}$, $d_2=2.8 \text{ c.c.}$) and $d_{\min \text{ diff}} = (d_2-d_1)_{\min} = 0.17 \text{ c.c.}$ (for $d_1=2.2 \text{ c.c.}$, $d_2=2.37 \text{ c.c.}$). $d_{\max \text{ diff}}$ and $d_{\min \text{ diff}}$ are used in (d_2-d_1) in Eqs (22) to (24) in calculating optimum values of μ of the diapiric salts.

- H: height of the diapiric column/channel; 10km and 8km for the Hormuz- (Koop and Stonely⁵) and the Namakdan diapir (Bahroudi & Talbot⁶), respectively.
- t: span of diapirism for the Hormuz- and the Namakdan diapirs. $t=10^4$ yrs (Bruthans et al.¹).

Namakdan salt diapir is shown by parabolic velocity profile. (Such extrusion geometry has been deciphered by Bruthans et al¹) Not to scale. See text for discussions and derivations.

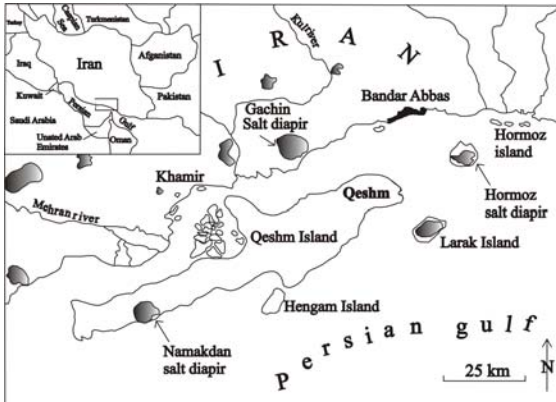


Figure 1. Geographic locations of the Hormuz- and the Namakdan islands in the Persian Gulf. Dark areas represent exposed salt diapirs. Reproduced from Bruthans et al¹.

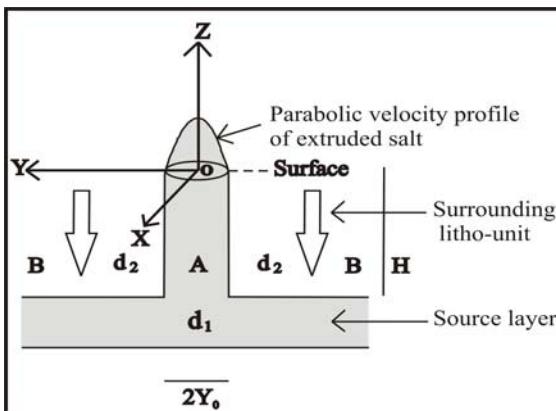


Figure 2. 'A' is a vertical cylinder with length 'H' and diameter ' $2Y_0$ '. 'A' is connected at the base with a horizontal channel, and they are full of Newtonian viscous fluids with density d_1 . The horizontal channel is under compression by an overlying fluid column 'B' with density d_2 . The hollow arrows indicate downward pressure exerted by the fluid in cylinder 'B'. Fluid in 'A' represents the Hormuz- and the Namakdan diapir salts in Tables-1, and -2 respectively. The extrusion of the Hormuz- and the

Table 1. Calculation of viscosity of salt of the Hormuz diapir considering (i) its elliptical planform; (ii) the rate of upward flow $U_z(x,y,t)$ & respective coordinate (x,y) (obtained from Fig. 2 and Fig. 9a respectively, of Bruthans et al.¹); & (iii) $d_{\max \text{ diff}}=0.8$ and $d_{\min \text{ diff}}=0.17$. Out of 28 calculated values of viscosities, the optimum values (8.75×10^{20} Pa s $\sim 10^{21}$ Pa s and 10^{18} Pa s respectively), are shown in bold.

Sample	Calculated from Fig. 2 of Bruthans et al (2006); considering diapir center as origin		Calculated from Fig. 9a of Bruthans et al (2006)	Calculation of viscosity (μ) using eqn (22)	
	'x' ordinate (in km)	'y' ordinate (in km)	Uplift rate $U_z(x,y,t)$ (in mm.y^{-1}) in eqn (22)	For $d_{\max \text{ diff}}=0.8$ c.c.	For $d_{\min \text{ diff}}=0.17$ c.c.; at $d_1=2.2$ c.c.
				μ_{\max} (in Pa s)	μ_{\min} (in Pa s)
H ₃	+0.39	+1.17	5.00	1.29×10^{20}	2.67×10^{19}
				1×10^{18}	1.1×10^{18}
H ₄	-0.44	+1.5	4.27	2.56×10^{20}	5.4×10^{19}
				1×10^{18}	1.04×10^{18}
H ₇	+0.50	+1.89	2.50	1.74×10^{20}	3.6×10^{19}
				1×10^{18}	1.1×10^{18}
H ₈	-1.5	+0.61	5.7	1.08×10^{20}	2.2×10^{19}
				1×10^{18}	1.1×10^{18}
H ₂	-1.83	0.83	4.7	8.75×10^{20}	1.85×10^{20}
				1×10^{18}	1.03×10^{18}
H ₁	-3.05	-0.47	2.2	1.52×10^{20}	3.2×10^{20}
				1×10^{18}	1.1×10^{18}
H ₅	-2.83	-0.11	4.7	8.82×10^{18}	1.8×10^{18}
				1×10^{18}	1.1×10^{18}

Table 2. Calculation of viscosity (μ) of salt of the Namakdan diapir considering (i) its planform as circular and taking the major- (7km) and minor axes (6.8km) as the diameters, in both sets of calculations; (ii) the y_1 value as obtained from Fig. (9b) of Bruthans et al.¹ is written in a column; and (iii) the density parameters, $d_{\max \text{ diff}}$ and $d_{\min \text{ diff}}$, as per caption of Table-1. Eqn (23) is used to calculate μ . The optimum of 44 calculated viscosities (6.5×10^{20} Pa s $\sim 10^{21}$ Pa s and 1.15×10^{17} Pa s $\sim 10^{17}$ Pa s respectively), are shown in bold in the table.

From Fig. 9b of Bruthans et al. ¹			Salt viscosity (μ) calculated using eqn (23)			
Sample	Dist. from salt diapir center (m) = y_1 in eqn (23)	Uplift rate (mm. y^{-1}); U_z (y ₁ ,t) in eqn (23)	For $2y_0=7\text{km}$		For $2y_0=6.8\text{km}$	
			For $d_{\max \text{ diff}}$	For $d_{\min \text{ diff}}$	For $d_{\max \text{ diff}}$	For $d_{\min \text{ diff}}$ c.c.
			μ_{\max} (in Pa s)	μ_{\min} (in Pa s)	μ_{\max} (in Pa s)	μ_{\min} (in Pa s)
N _{1/2}	2250	4.7	8.9×10^{19} 1.2×10^{18}	1.99×10^{20} 1.5×10^{18}	7.39×10^{19} 1.15×10^{17}	1.67×10^{20} 3.3×10^{19}
N _{2/1}	2250	4.1	1.09×10^{20} 1.2×10^{18}	2.1×10^{19} 1.4×10^{18}	1.9×10^{20} 3.8×10^{19}	1.97×10^{19} 1.7×10^{18}
N _{7a}	3310	2.55	3.1×10^{19} 1.2×10^{18}	6.5×10^{20} 2.95×10^{18}	1.38×10^{20} 1.2×10^{18}	No real solution
N _{7b}	3310	2.45	3.1×10^{19} 1.2×10^{18}	5.3×10^{18} 8.6×10^{17}	1.38×10^{20} 1.2×10^{18}	No real solution
N _{6d}	2800	3.75	6.03×10^{18} 1.5×10^{18}	1.66×10^{19} 1.4×10^{18}	5.89×10^{20} 1.15×10^{18}	1.16×10^{19} 1.18×10^{18}
N _{6x}	2800	3.0	7.6×10^{18} 1.4×10^{18}	1.86×10^{19} 1.4×10^{18}	7.39×10^{19} 1.15×10^{18}	1.67×10^{19} 3.15×10^{17}

ACKNOWLEDGMENTS

SM thanks R. Govindarajan and K.C. Sahu (JNCASR, India) for teaching fluid mechanics and acknowledges 'Swedish Institute's 'Guest Scholarship' during 2005-2006 to carry out this work in the Hans Ramberg Tectonic Lab, Uppsala University. HAK was supported by the 'Swedish Research Council'. R. Chakraborty formatted the manuscript.

REFERENCES

1. Bruthans, J., Filippi, M., Geršl, M., Zare, M., Melková, J., Pazdur, A., Bosák, P. (2006). "Holocene marine terraces on two salt diapirs in the Persian Gulf, Iran: age, depositional history and uplift rates." *Journal of Quaternary Science*, **21**, 843-857.

2. Papanastasiou, C.T., Georgiou, G. C., Alexandrou, A.N.(2003). "Viscous Fluid Flow", CRC Press, Florida.

3. Weinberger, R., Lyakhovsky, V., Baer, G., Begin, Z.B. (2006). "Mechanical modeling and InSAR measurements of Mount Sedom uplift, Dead Sea basin: Implications for effective viscosity of rock salt." *Geophysics Geochemistry Geosystems* **7**, Q05014, DOI: 10.1029/2005GC001185.

4. Mizutani, S. (1984). "Salt Domes in the Gulf Coast". In: Uemura, T., Mizutani, M. (Eds), Geological Structures. John Wiley & Sons, Chichester, pp. 106-133.

5. Koop, W.J., Stonely, R. (1982). "Subsidence history of the Middle East Zagros basin, Permian to recent". In: Kent,

D.P., McKenzie, C.A.W. (Eds),
*Philosophical Transactions of the Royal
Society, London*, **305**, 149-168.

6. Bahroudi, A., Talbot, C. J. (2003). "The
configuration of the basement beneath the
Zagros basin." *Journal of Petroleum
Geology*, **26**, 257-282.